Journal of Thermal Analysis and Calorimetry, Vol. 91 (2008) 2, 551–557

THERMAL DECOMPOSITION OF AMMONIUM PERCHLORATE BASED MIXTURE WITH FULLERENES

X. Han[1], *Y. L. Sun*[1], *T. F. Wang*[1], *Zh. K. Lin*[1], *Sh. F. Li*[1*], *F. Q. Zhao*[2], *Z. R. Liu*[2], *J. H. Yi*[2] *and X. N. Ren*[2]

[1]Department of Chemical Physics, University of Science and Technology of China, Hefei 230026, P.R. China
[2]Xi'an Modern Chemistry Research Institute, Xi'an 710065, P.R. China

The effects of fullerenes, including fellerene soot (FS), extracted fullerene soot (EFS) and pure C_{60} on the thermal decomposition of ammonium perchlorate (AP) compared with traditional carbon black (CB) catalyst has been studied by employing thermogravimetry (TG), differential thermal analysis (DTA), infrared spectroscopy (IR) and ignition temperature experiments. The results showed that the addition of CB and FS to AP reduced the activation energy as well as the temperature at maximum decomposition rate, but that of EFS and pure C_{60} had little effect on the thermal decomposition of AP, and among all catalysts, FS was the best one.

Keywords: *ammonium perchlorate, fullerene, thermal decomposition*

Introduction

The discovery of C_{60} in 1985 [1] and the development of mass production of fullerenes [2] have stimulated intensive research efforts. The extensive investigation of physical and chemical properties has revealed its application to the fields of superconductivity [3], magnetism, photoconductivity [4] and propellants [5]. The thermochemistry of C_{60} and C_{70} fullerene solvates has recently reported by Korobov [6].

Ammonium perchlorate (AP) has long been of chemical interest as oxidizers, and has found excellent application in propellants, explosives, and pyrotechnics. The thermal decomposition characteristics influence the combustion behavior of the propellants. The catalytic decomposition of AP by different additives has ever been well studied by Boldyreva [7] and Jacobs [8]. Our research group has reported the catalytic thermal decomposition of AP by different catalysts [9, 10]. The aim of this research work is to investigate the catalysis of fullerenes on thermal decomposition of AP by using thermal analysis and IR techniques in order to reveal the influence of fullerenes on the combustion of solid propellants.

Experimental

Materials

The powdered sample of AP power (technical pure) was sieved to the grain diameters of 80–90 μm. Fullerene soot (FS) (comprised of 10% fullerenes and 90% carbon black) is the primary product of electric arc evaporation of graphite under helium atmosphere. Extracted fullerene soot (EFS) contains about 80% C_{60} and 20% C_{70} and the purity of C_{60} is 99.9%. Mixtures of fullerenes and AP were prepared by carefully mixing of the two components in a polished porcelain container with acetone as the dispersant. All materials were prepared carefully in order to ensure the purity of the sample surface.

Methods

Thermogravimetry, differential thermogravimetry (TG-DTG) curves were obtained on a model Shimadzu TGA-50 in the temperature range of 20–600°C. Thermal decomposition patterns of the mixtures were studied thermogravimetrically at a heating rate of 10°C min^{-1} in nitrogen atmosphere with a flow rate of 25 mL min^{-1}. The thermal decomposition kinetic parameters of the samples were obtained from TG-DTG analysis at four different heating rates, 5, 10, 20 and 25°C min^{-1}. The sample masses were about 2 mg and the samples were placed in aluminum oxide crucible.

Differential thermal analysis (DTA) curves were obtained on a model Shimadzu DTA-50 in the temperature range of 20–600°C. The heating rate was also 10°C min^{-1} in nitrogen atmosphere with a flow rate of 25 mL min^{-1}. The sample masses were about 5 mg and the samples were placed in aluminum oxide crucible without cover.

---

[*] Author for correspondence: lsf@ustc.edu.cn

1388–6150/$20.00

Akadémiai Kiadó, Budapest, Hungary
Springer, Dordrecht, The Netherlands

Infrared spectroscopy (IR) spectra were obtained from 60SXR Fourier transform infrared spectroscopy apparatus with a heating rate of 50°C s^{-1}. The sample mass was about 1 mg and the scan rate was 5 files s^{-1}, 2 scans $file^{-1}$. The detector was MCT-A. All the volatile and gaseous decomposition products which have an infrared activity, will be recorded.

Ignition temperature was detected with a tube furnace at ambient temperature under a pressure of 1 atm. The thermocouple was placed on the top of the sample that was directly put in the inner wall of the tube furnace. The sample with a dimension of 1 cm×0.5 cm×0.5 cm was placed at the position that is about 1 cm to the end-tip of the tube furnace.

Results and discussion

The thermal decomposition of AP-additive mixtures

The representative TG and DTA curves of AP-additive mixtures are shown in Figs 1 and 2. The initiative decomposition temperature (IDT), step of low temperature decomposition (LTD) and step of high temperature decomposition (HTD) of AP and AP-additive mixtures are listed in Tables 1 and 2, respectively.

In TG curves, AP exhibits two major steps of mass loss, the low-temperature decomposition process and high-temperature decomposition process. The low-temperature decomposition covers a temperature region from 260 to 320°C, in which AP undergoes an autocatalytic reaction with about 26% decomposition. The high-temperature decomposition demonstrates a mass loss of about 74% in the temperature region of 340 to 410°C. From Fig. 1 and Table 1, one can see that the IDT are obviously advanced by all catalysis. Especially, the IDT of AP is advanced about 32°C with addition of 5% FS. But for the other catalysts, the IDT are almost the same and are advanced about 10°C. The low-temperature decomposition of AP is almost unaffected by mixing the AP with 5% EFS or 5% C_{60}, while the high-temperature decomposition is slightly catalyzed and the peak temperatures of maximum decomposition rate are advanced about 10°C. The high-temperature decomposition of AP is evidently catalyzed with addition of 5% CB or 5% FS and the high-temperature decomposition peak temperatures are advanced about 45°C. From above-mentioned experiments the samples containing FS has the best effects to improve thermal decomposition of AP, this is mostly because FS has larger specific area than other catalysts.

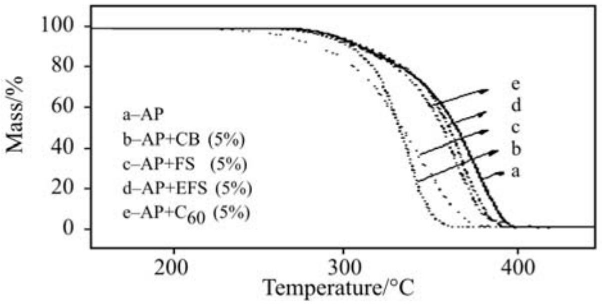

Fig. 1 The TG curves of AP-additive mixtures

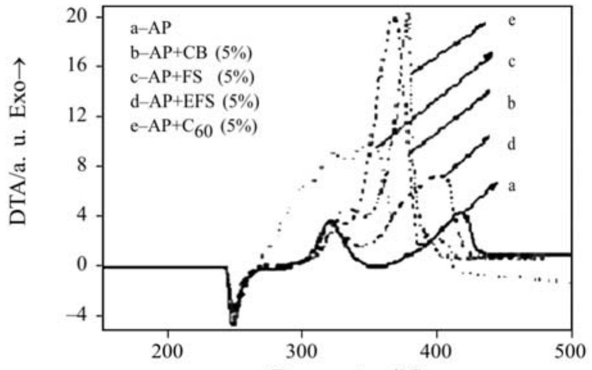

Fig. 2 The DTA curves of AP-additive mixtures

Table 1 The TG-DTG data of AP-additive mixtures

Samples	IDT/°C	LTD/°C	HTD/°C
AP	261.6	308.2	381.1
AP+5% CB	250.6	281.7	337.5
AP+5% FS	229.4	273.8	335.8
AP+5% EFS	253.4	305.4	370.7
AP+5% C_{60}	252.9	309.5	371.2

Table 2 The DTA data of AP-additive mixtures

Samples	CMT/°C	LTD/°C	HTD/°C	TDS/°C
AP	247.3	318.2	415.3	–
AP+5% CB	249.5	321.7	365.3	392.8
AP+5% FS	248.9	321.2	347.0	393.2
AP+5% EFS	246.8	321.5	399.6	506.1
AP+5% C60	248.7	330.7	375.8	–

CMT – crystal modification temperatures;
TDS – step of the third decomposition stage

From Fig. 2, we can see that the crystal modification process is endothermic and the first and second decomposition stages, which are assigned to low-temperature decomposition and high-temperature decomposition respectively, are exothermic. The endothermic event is quite similar for the different samples and for all of them the peak temperatures are almost the same. This event occurs around 248°C and it represents a phase transition of AP from the orthorhombic to the cubic form. The first exothermic peak temperatures of AP, AP with 5% CB, AP with 5% FS and AP with 5% EFS are almost the same, but the peak temperature of AP with 5% C_{60} is 13°C higher than pure AP. The second exothermic peak temperature of AP is obviously advanced by all the catalysts in which FS shows the best catalytic effect, about 68°C lower than pure AP.

It is interesting that in the DTA curve of AP with 5% CB and AP with 5% FS there is an exothermic peak at 393°C. One possible reason is that at high temperature the carbon can react with NO molecular which is one product in the thermal decomposition of AP [11].

$$C+NO \rightarrow CO+\frac{1}{2}N_2$$

$$\frac{1}{2}C+NO \rightarrow \frac{1}{2}CO_2+\frac{1}{2}N_2$$

Since the two reactions are exothermic, therefore, an exothermic peak appears at 393°C in the DTA curve of AP with 5% CB and AP with 5% FS respectively, which can be verified in the infrared spectra of AP with 5% CB. With the addition of CB and FS, C=O absorbance peak can be detected while this peak is not found in the decomposition process of pure AP. The mass loss of this process is very small, so we do not observe the peak of mass loss in TG curves.

And in the DTA curves of AP with 5% EFS there is an exothermic peak at about 506°C. Because the C_{70} and higher carbon fullerene in EFS are unstable and could easily decompose to carbon black [12]. This process is exothermic and occurs at about 500°C. In this process there is not any volatile products, so no mass loss is observed.

The thermal decomposition of AP with different CB or FS contents

To elucidate the features of the catalytic effect of CB and FS catalysts, we studied the decomposition of AP with different CB or FS contents in more detail. The TG curves of AP with 3, 5, 8 and 10% CB or FS contents at a heating rate of 10°C min^{-1} in the temperature range of 20–600°C are shown in Figs 3 and 4, respectively. The maximum decomposition peak temperatures of the two stages of AP with different contents of CB or FS are listed in Table 3.

According to the results above, both CB and FS are shown evidently catalytic effect on thermal decomposition of AP. When comparing the same content of CB catalyst to FS catalyst, one can see the effect of FS on thermal decomposition of AP is more significant. Addition of 3% CB to AP do not have an effect on the IDT while the IDT is advanced about 25°C with addition of 3% FS, meanwhile, the IDT of AP with 5, 8 and 10% FS is about 21, 23 and 27°C lower than that of AP with 5, 8 and 10% CB respectively. The addition of 3% CB to AP acts strongly on the LTD and HTD of AP, and it suppresses the LTD and promotes the HTD of AP. The LTD is postponed about 28°C while the HTD is advanced about 24°C. While addition of 5, 8 and 10% CB to AP, they promote not only the IDT but also the LTD and HTD of AP, especially, additions of 8 and 10% CB make the LTD and HTD coincident.

It is interesting that the effect of 3% FS is different from 3% CB, addition of 3% CB to AP does not affect the IDT but it suppresses the LTD and promotes the HTD of AP. While addition of 3% FS promotes not only the IDT but also the LTD and HTD of AP. Addition of 5, 8 and 10% FS to AP is the same as

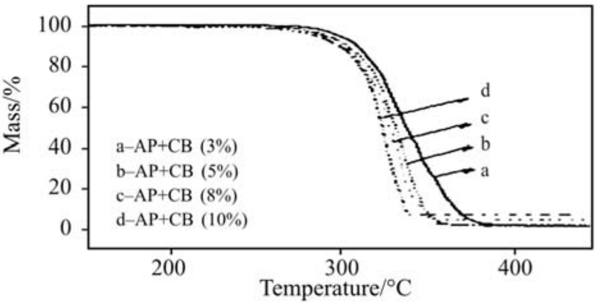

Fig. 3 The influence of different CB contents on thermal decomposition of AP

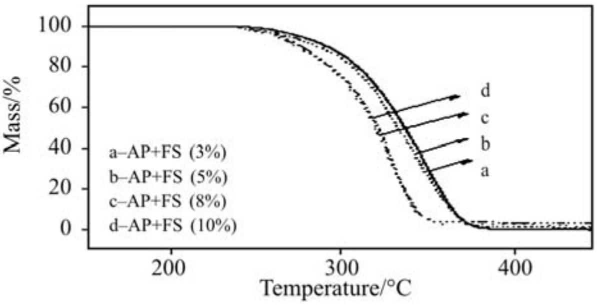

Fig. 4 The influence of different FS contents on thermal decomposition of AP

Table 3 The TG data of AP with different CB or FS contents

Samples	IDT/°C	LTD/°C	HTD/°C
AP	261.6	308.2	381.1
AP+3% CB	263.3	336.1	356.7
AP+5% CB	250.6	281.7	337.5
AP+8% CB	250.6	–	333.0
AP+10% CB	245.3	–	329.0
AP+3% FS	236.6	271.6	353.4
AP+5% FS	229.4	273.8	335.8
AP+8% FS	227.8	–	332.3
AP+10% FS	218.1	–	331.1

*The peaks of LTD and HTD are coincident and the mass loss of HTD can not be measured that of CB, but they all showed better catalytic effects than 3% content of CB or FS.

Kinetics of decomposition of AP with 5% CB and 5% FS additives

A specific feature of thermal decomposition of AP is extremely sensitive to the action of various additives. With the objection to obtain the kinetics of the high-temperature decomposition of AP with additives, we studied the influences of four heating rates on thermal decomposition of AP with CB and FS additives. In order to make the comparison obviously, we used 5% content of CB and FS. The basic equation used to estimate the activation energy of AP-additive mixtures decomposition is:

$$\log\beta = -2.315 + \log\left[\frac{AE}{RF(\alpha)}\right] - 0.4567\frac{E}{RT}$$

(Ozawa method [13])

where β is the programmed heating rate (°C min^{-1}), *E* is the activation energy, *A* is the pre-exponential factor and *R* is the gas constant, $F(\alpha)$ is fitted as a function of conversion degree (α) and *T* is the temperature at a constant conversion degree, which in the TG curve is the temperature at α=0.5. Thus, as the heating rate is increased, the reaction peak shifts to higher temperature and therefore an estimation of the activation energy may be made. The pre-exponential factor *A* is deduced in the first order using the equation:

$$A = \left(\frac{bE}{RT_{\max}^{2}}\right)\exp\left(\frac{E}{RT}\right)$$

The activation energy of AP with 5% CB is slightly larger than that of AP with 5% FS. In the presence of FS the activation energy of the thermal decomposition reaction is reduced by 37% as shown in Table 4. It is seen that the maximum rate constants are determined by the following expressions:

with CB, $K=3.18\cdot10^{16}\exp(-192300/RT)\ \mathrm{min}^{-1}$
with FS, $K=3.02\cdot10^{15}\exp(-185800/RT)\ \mathrm{min}^{-1}$

IR analysis

The infrared spectroscopic measurements of the gaseous products were conducted under 1 atmosphere of nitrogen pressure. The results of the thermal decomposition studies suggest that the course of mass loss of AP consists of several independent processes. Thus, it would be possible to detect the products produced in each process by selecting the heating rate and the upper limit of temperature properly. An infrared spectroscopic approach enables one to obtain direct information about the molecular structure and to assign to unknown products with high-boiling temperature. Typical infrared spectra are shown in Fig. 5 for the wave number from 800 to 4000 cm^{-1}. All the measurements are conducted in a flowing nitrogen atmosphere (40 mL min^{-1}). The sample masses were about 1 mg and heated to 500°C using a heating rate of 50°C s^{-1}.

In Fig. 5a, the 3276 and 1424 cm^{-1} can be assigned to N–H stretching vibration and N–H bending band in the ammonia, the 2248 cm^{-1} can be related to N_2O atmosphere, the 1634 and 1599 cm^{-1} are belonged to NO_2 atmosphere, the 1085 and 633 cm^{-1} are assigned to ClO_4^- anion which occurred at 270°C. No C=O vibration peak is found during the whole decomposition process of AP, the appearance of N–H and ClO_4^- vibration absorbance peaks elucidates that the thermal decomposition of AP is based on the proton transfer from ammonia cation to perchloric acid anion.

However, in Fig. 5b some new absorption peak is observed at 2345 (belonged to CO_2), 2201 (belonged to CO), 1715 (belonged to HCHO), 1311 and 878 cm^{-1} (belonged to HNO_3), which do not find in the decomposition process of pure AP.

In Fig. 5c the absorbance peak of N–H stretching vibration is not obvious but the absorbance peak that assigned to CO_2 is very strong and there is not any new peak different from that of AP with 5% CB. In Fig. 5d there is not any new peak different from Fig. 5c.

Ignition temperature measurement

The ignition temperatures of pure AP, AP with 5% CB, AP with 5% FS, AP with 5% EFS and AP with 5% C_{60} mixtures are shown in Table 5. The sample masses are about 1 g with a dimension of 1 cm×0.5 cm×0.5 cm during one experiment. The experiments were carried out in a tube furnace and the voltage was regulated to 172.5 V through a transformer with a voltage range of 0~250 V. The samples were placed at a distance of 1 cm to the rear of the tube furnace.

Table 4 Kinetic parameters for the thermal decomposition of AP-additive mixtures

Samples	Activation energy/kJ mol^{-1}	Pre-exponential factor/min^{-1}	Correlation coefficient; *R*
AP	293 [13]		
AP+5% CB	192.3	$3.18\cdot10^{16}$	0.986
AP+5% FS	185.8	$3.02\cdot10^{15}$	0.999

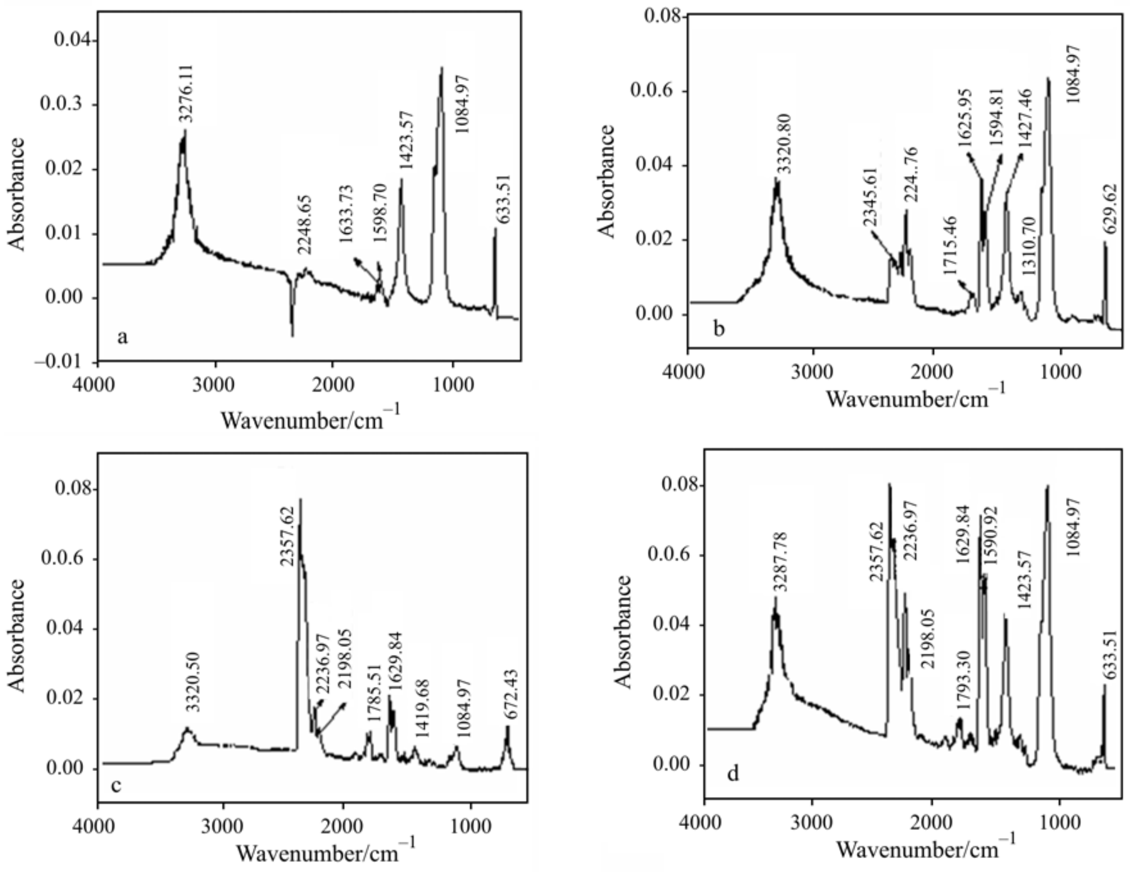

Fig. 5 IR spectra of the products of AP-additive mixture obtained at t=6.0 s. Samples used: a – pure AP, b – AP+5% CB, c – AP+5% FS, d – AP+5% EFS

Table 5 The ignition temperatures (T_{ign}) of AP-additive mixtures

T_{ign}	AP	AP+5% CB	AP+5% FS	AP+5% EFS	AP+5% C_{60}
Experiment 1/°C	304.4	289.6	258.8	298.5	295.6
Experiment 2/°C	305.3	295.5	256.2	300.1	294.8
Average/°C	304.9	292.6	257.5	299.3	295.2

The results show that all catalysts can decrease the ignition temperature of AP. The ignition temperatures of AP with 5% CB, 5% EFS and 5% C_{60} are advanced by 12.3, 5.6 and 9.7°C respectively. Among all catalysts, FS gives the best catalytic effect. Addition of 5% FS to the pure AP makes the ignition temperature advanced by 47.4°C.

Catalysis mechanisms

Boldyrev [14] reviewed the thermal decomposition of AP and displayed the mechanism of thermal decomposition of AP, based on the proton transfer from cation to anion that is reported everywhere [15–20]. The following scheme represented the thermal decomposition mechanisms of AP.

$$\begin{gathered}\mathrm{NH_4ClO_4} \Leftrightarrow \mathrm{H_3N{-}H{-}ClO_4}\\ \Updownarrow\\ \mathrm{NH_3{-}HClO_4}\\ \Updownarrow\\ \mathrm{NH_3}(g)\mathrm{+HClO_4}(g)\end{gathered}$$

Decomposition or sublimation starts with proton transfer from ammonium ion to perchlorate ion. First, molecular complex NH_3–H–ClO_4 is formed; then it decomposes into NH_3 and $HClO_4$.

The process of low-temperature thermal decomposition starts with the formation of nuclei. The nuclei are cavities that are formed as a result of proton transfer filling filled with the gaseous products of decomposition of AP. Centers of partial decomposition, according to Raevsky [21] are formed as a result of proton transfer. The key factor for understanding the process of thermal decomposition of ammonium perchlorate is the presence of proton trap, which is ClO_3 radical:

$$NH_4^+ + ClO_4^- \rightarrow NH_3 + HOClO_3$$
$$HOClO_3 \rightarrow HO + ClO_3$$

The ClO_3 radical can react with ammonia to give a mixture of $HClO_3$ molecular and NH_2 radical. The $HClO_3$ is unstable and decomposes to ClO_2 that is detected as an intermediate during thermal decomposition of AP.

$$ClO_3 + NH_3 \rightarrow NH_2 + HOClO_2$$
$$HOClO_2 \rightarrow OH + ClO_2$$

The formation of nitric dioxide and nitric acid is possible through the following ways:

$$ClO_3 + NH_2 \rightarrow H_2O + ClNO_2$$
$$ClNO_2 \rightarrow Cl + NO_2$$
$$NO_2 + H_2O \rightarrow HNO_3 + NO$$

Firstly, one H_2O molecular and one $ClNO_2$ radical are formed through the reaction of ClO_3 radical and NH_2 radical, secondly, $ClNO_2$ radical decomposes to Cl and NO_2, finally, the NO_2 farther reacts with H_2O molecular to form HNO_3 and NO.

The formation of nitric monoxide and nitrous oxide is possible through the following ways:

$$NO_2 + H_2O \rightarrow HNO_3 + NO$$
$$ClNO_2 + NH_3 \rightarrow HCl + H_2NNO_2$$
$$H_2NNO_2 \rightarrow N_2O + H_2O$$
$$ClO_2 + NH_2 \rightarrow ClNO + H_2O$$

$$ClNO \rightarrow NO + Cl$$
$$OH + NH_4 \rightarrow H_2O + NH$$
$$ClO_2 + NH \rightarrow ClO + HNO$$
$$HNO + Cl \rightarrow NO + HCl$$

$$HNO + OH \rightarrow NO + H_2O$$
$$HNO + HNO \rightarrow N_2O + H_2O$$

The formation of carbon oxide and formaldehyde can be possible through the following steps:

$$C + NO \rightarrow CO + \frac{1}{2}N_2$$
$$\frac{1}{2}C + NO \rightarrow \frac{1}{2}CO_2 + \frac{1}{2}N_2$$
$$OH + CO_2 \rightarrow HCOH + O$$

Conclusions

- Each catalyst lowers the IDT and HTD of AP. CB and FS also lower the LTD of AP.
- The more contents of FS and CB catalysts, the better the catalytic effect will be.
- The catalytic effect of FS is the best among all the catalysts.

Acknowledgements

We gratefully acknowledge the National Natural Science Foundation of China (No. 50476025) and National Defence Key Laboratory supports for this research.

Nomenclature

FS	fullerene soot
EFS	extracted fullerene soot
AP	ammonium perchlorate
CB	carbon black
DTG	differential thermogravimetry
DTA	differential thermal analysis
IR	infrared spectroscopy
IDT	initiative decomposition temperature
HTD	step of high temperature decomposition
LTD	step of low temperature decomposition
CMT	crystal modification temperatures
TDS	step of the third decomposition stage

References

1 H. W. Kroto, J. R. Heath, S. C. O'Brien, R. F. Curland and R. E. Smalley, Nature, 318 (1985) 162.

2 W. Kratschmer, L. D. Lamb, K. Fostiropoulos and D. R. Huffman, Nature, 347 (1990) 354.

3 A. F. Hebard, M. J. Rosseinsky, R. C. Haddon, D. W. Murphy, S. H. Glarum, T. T. M. Plastra, A. P. Ramirez and A. R. Kortan, Nature, 350 (1991) 600.

4 Y. Wang, Nature, 356 (1992) 585.

5 B. E. Greiner, R. A. Frederick Jr. and M. D. Moser, J. Propulsion Power, 19 (2003) 713.

6 M. V. Korobov, A. M. Parfenova, P. A. Dorozhko, N. A. Kiseleva and P. V. Dolgov, J. Therm. Anal. Cal., 84 (2006) 259.

7 A. V. Boldyreva, B. N. Bezrukov and V. V. Boldyrev, Kinetics Catal., 8 (1967) 299.

8 P. W. Jacobs and H. M. Whithead, Chem. Rev., 4 (1969) 551.

9 S. F. Li, X. Han, Y. L. Sun, T. F. Wang and F. Q. Zhao, 41st AIAA/ASME/SAE/ASEE Joint Propulsion Conference and Exhibit, Arizona, 10–13 March 2005, Tucson 2005.

10 J. Zhi, W. Tian-Fang, L. Shu-Fen, Z. Feng-Qi, L. Zi-Ru, Y. Cui-Mei, L. Yang, L. Shang-Wen and Z. Gang-Zhui, J. Therm. Anal. Cal., 85 (2006) 315.

11 S. C. Tsang, Y. K. Chen and M. L. H. Green, Appl. Catal. B: Environmental, 8 (1996) 445.
12 I. Mochida, M. Egashira, H. Koura, K. Dakeshita and S. H. Yoon, Carbon, 33 (1995) 1186.
13 T. Ozawa, J. Thermal Anal., 2 (1970) 301.
14 V. V. Boldyrev, Thermochim. Acta., 443 (2006) 1.
15 B. S. Svetlov and V. A. Koroban, Kinet. Katal., 8 (1967) 456.
16 B. S. Svetlov and V. A. Koroban, Fizika Goreniya Vzryva., 6 (1970) 12 (in Russian).
17 L. Dauerman, H. Kimmel and Y. Wu, Combust. Sci. Technol., 5 (1972) 129.
18 V. V. Boldyrev, Yu. P. Savintsev, T. V. Mulina and G. V. Shchetinina, Kinet. Katal., 11 (1970) 1131.
19 Y. P. Savintsev, T. V. Mulina and V. V. Boldyrev, Combustion Explosion, 756 (1972) (in Russian)
20 V. V. Boldyrev, Dokl. AN SSSR., 181 (1968) 1406.
21 A. V. Raevsky, G. B. Manelis, Ed., Chernogolovka: Institute of Chemical Physics AS USSR., 30 (1981).

Received: April 12, 2007
Accepted: April 17, 2007
OnlineFirst: October 13, 2007

DOI: 10.1007/s10973-007-8290-6